

# DDPWM Based Control of Matrix Converters

Yulong Li<sup>\*</sup>, Nam-Sup Choi<sup>†</sup>, and Byung-Moon Han<sup>\*\*</sup>

<sup>\*</sup>Division of Electro Electric Systems, Hyundai Heavy Industries Co., LTD., Ulsan, Korea

<sup>†</sup>Division of Electric., Electron. Communication & Computer Eng., Chonnam National University, Yeosu, Korea

<sup>\*\*</sup>Dept. of Electrical Engineering, Myongji University, Yongin, Korea

## ABSTRACT

In this paper, pulse-width modulation (PWM) control strategy of various topologies of matrix converters is presented, which is based on direct duty ratio PWM (DDPWM). Because the DDPWM method has the characteristics of the inherent per-phase modular structure, it can be effectively applied to single-phase, two-phase and three-phase four-leg matrix converters as well as the common three-phase to three-phase matrix converter. Also, this paper treats command generation method in each matrix converter. The feasibility and validity of the proposed method are verified by experimental results.

**Keywords:** Matrix converter, Direct duty-ratio PWM, AC-AC power conversion

## 1. Introduction

Recently, matrix converters are getting more attention in ac-ac power processing systems that require smaller size, higher power density and easier maintenance [1-4]. As well known, the matrix converters have attractive characteristics such as sinusoidal input currents, a controlled input power factor, regeneration capability as well as the basic function to produce magnitude-frequency controllable output voltages.

The performance of matrix converters is strictly dependent upon the pulse-width modulation (PWM) strategy employed

to control the bidirectional switches. Since the introduction of the matrix converter, various and numerous modulation methods have been developed to date. In [5] and [6], off-line global duty ratio functions are mathematically derived, which can be modulated by a carrier signal [5-6]. This method requires a formidable amount of complex calculations in the stage of implementation. Space vector PWM (SVPWM) for a matrix converter explores a more systematic approach to understand the operation of the matrix converter [7-8]. However, the SVPWM is far from intuitive and requires lookup tables with the previously initialized and stored switching patterns.

Carrier based PWM may be the latest modulation strategy for matrix converters [9-11]. The carrier based PWM will employ the carrier and reference signals and can be implemented without complex calculations and lookup tables. The method in [9], however, involves proper offset voltages and discontinuous carrier signals which imply relatively indirect understanding of

---

Manuscript received Dec. 4, 2008; revised April 20, 2009

<sup>†</sup> Corresponding Author: nschoi@chonnam.ac.kr

Tel: +82-61-659-3311, Fax: +82-61-659-3319, Chonnam Univ.

<sup>\*</sup>Division of Electro Electric Systems, Hyundai Heavy Industries Co., LTD., Ulsan, Korea

<sup>†</sup>Division of Electric., Electron. Communication & Computer Engineering, Chonnam National University, Yeosu, Korea

<sup>\*\*</sup>Dept. of Electrical Engineering, Myongji Univ., Yongin, Korea

modulation processes. Also, the modulation algorithm suffers from additional complicated modification in order to get a maximum gain of 0.866. Moreover, this method can not be applied to matrix converter topologies with a neutral connection between input and output neutrals.

In [10], a carrier based PWM strategy, called direct duty ratio PWM (DDPWM), is presented for the 3-phase to 3-phase matrix converter, which does not require the reference offset and employs a continuous triangular carrier waveform. The desired output phase voltages can be synthesized by utilizing the input phase voltages based on per-output-phase average concept over one switching period, i.e., per-carrier cycle. A maximum gain of 0.866 can be simply obtained by injecting third harmonic components to output voltage references in the three phase system. In [11], the DDPWM method is extended in order to apply it to the various matrix converter topologies such as 3-phase to single-phase matrix converters with single-leg or 2-leg, 3-phase to 2-phase matrix converters with 2-leg or 3-leg, 3-phase to 3-phase matrix converter with 4-leg.

In this paper, a systematic method to generate the reference signals in various matrix converters is presented. Before the DDPWM is applied to synthesize the output voltages, the per-phase output voltage references should be given at each switching time. The global minimum of the input voltage range is used to determine the output voltage magnitude. The feasibility and validity of the proposed DDPWM method applied in various matrix converters will be verified with simulation and experiment results.

## 2. Output Voltage Synthesis by DDPWM

Fig. 1 shows a leg configuration to implement a matrix converter, which can be considered as a basic module to explain the DDPWM because the DDPWM was developed by using the concept of per-output-phase average over one switching period. In Fig. 1, *MX*, *MD* and *MN* denote the maximum, medium and minimum input phase voltages, respectively. During  $T_1$ , the line-to-line voltage between *MX* and *MN* is used, which is the maximum line-to-line voltage among three line-to-line input voltages at the sampling instant. During  $T_2$ , the second maximum line-to-line voltage that is the larger one in *MX* to *MD* and *MD* to *MN*, is used to obtain the output

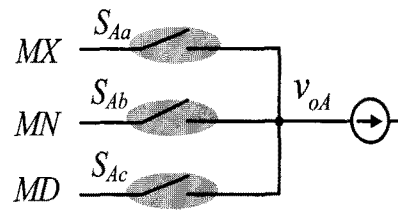


Fig. 1. A leg configuration for a matrix converter.

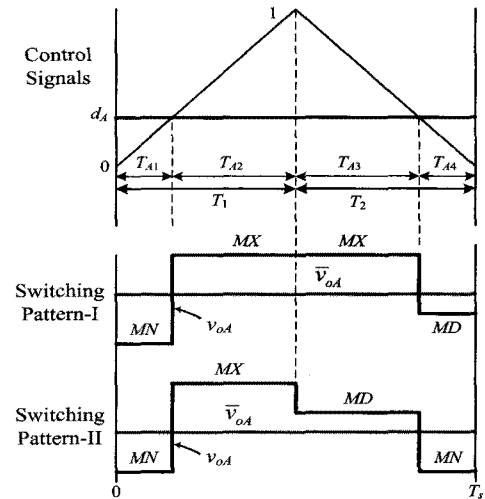


Fig. 2. Switching state in the case of switching pattern-I and switching pattern-II.

voltage. If  $MX-MD > MD-MN$ , *MX* to *MD* is used during  $T_2$  and the resultant switching pattern is named switching pattern-I. Otherwise, *MD* to *MN* is used during  $T_2$ , and it is named switching pattern-II.

Fig. 2 shows switching pattern-I and pattern-II for generating *A*-phase output voltage where a triangular carrier is compared with a duty ratio value,  $d_A$ . The output phase voltage can be changed from  $MN \rightarrow MX \rightarrow MD$  for switching pattern-I and  $MN \rightarrow MX \rightarrow MD \rightarrow MN$  for switching pattern-II. The four sub-intervals can be expressed as:

$$\begin{aligned} T_{A1} &= d_{A1} n T_s \\ T_{A2} &= (1 - d_{A1}) n T_s \\ T_{A3} &= (1 - d_{A1}) (1 - n) T_s \\ T_{A4} &= d_{A1} (1 - n) T_s \end{aligned} \quad (1)$$

where  $T_s$  is the switching frequency and  $n$  is defined by  $n = T_1 / T_s$  which involves the slope of the carrier.

It is found from Fig. 2 that the averaged value of  $v_{oA}$ ,  $\bar{v}_{oA}$ , can be approximated by:

$$\bar{v}_{oA} = \frac{1}{T_s} \int_0^{T_s} v_{oA} dt = \begin{cases} d_A(n \cdot MN - n \cdot MD + MD - MX) + MX & \text{for pattern-I} \\ d_A(MN - n \cdot MX - MD + n \cdot MD) + n \cdot MX \\ -n \cdot MD + MD & \text{for pattern-II} \end{cases} \quad (2)$$

By letting  $\bar{v}_{oA}$  be equal to the  $A$ -phase output voltage command,  $v_{oA}^*$ , that is  $\bar{v}_{oA} = v_{oA}^*$ , the duty ratio value,  $d_A$ , for the present switching period can be calculated as:

$$d_A = \begin{cases} \frac{MX - v_{oA}^*}{(MX - MD) + n(MD - MN)} & \text{if } (MX - MD) \geq (MD - MN) \\ \frac{n(MX - MD) + (MD - v_{oA}^*)}{n(MX - MD) + (MD - MN)} & \text{if } (MX - MD) < (MD - MN) \end{cases} \quad (3)$$

The gating signal of the bidirectional switches can be directly generated by considering Fig. 2. If the switching state of phase "A" is  $MX$  (or  $MD$ ,  $MN$ ), the output phase "A" is connected to the input phase whose voltage is  $MX$  (or  $MD$ ,  $MN$ ).

It should be noted that, when driving the duty ratio value,  $d_A$ , in equation (3), there was no consideration in the other leg's switching state. This means that the multiple output phases can be separately controlled to follow their references. This fact results in modular structure of the DDPWM. Therefore, it can be concluded that one can produce easily the duty ratio  $d_x$ , ( $x=1,2,\dots,m$ ) for each phase in 3-phase to  $m$ -phase matrix converter with  $m$ -leg (See Fig. 3) as given by:

$$d_x = \begin{cases} \frac{MX - v_{ox}^*}{(MX - MD) + n(MD - MN)} & \text{if } (MX - MD) \geq (MD - MN) \\ \frac{n(MX - MD) + (MD - v_{ox}^*)}{n(MX - MD) + (MD - MN)} & \text{if } (MX - MD) < (MD - MN) \end{cases} \quad (4)$$

where  $v_{ox}^*$  ( $x=1,2,\dots,m$ ) is the reference output voltages at  $x$ -phase.

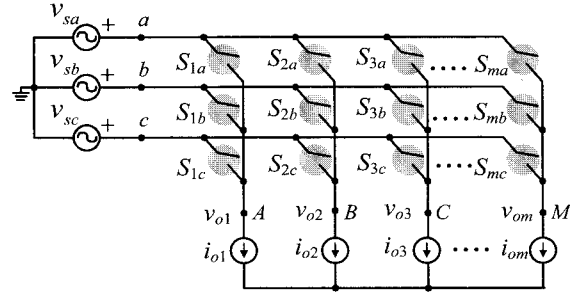


Fig. 3. Circuit configuration of a 3-phase to  $m$ -phase matrix converter with  $m$ -leg.

### 3. Generation of reference output voltage

In this section, the method of producing a reference output phase voltage is addressed for various matrix converter topologies. A phase voltage is synthesized by using three input phase voltages and the output voltage  $v_{ox}$  is fallen into the following range.

$$B_L(t) \leq v_{ox}(t) \leq B_U(t) \quad (5)$$

where  $B_L(t)$  and  $B_U(t)$  are the input voltage lower bound and input voltage upper bound, respectively. Also, the magnitude of input range,  $IR(t)$ , and the input range offset,  $IR_{offset}(t)$ , can be expressed by:

$$IR(t) = B_U(t) - B_L(t) \quad (6)$$

$$IR_{offset}(t) = \frac{B_U(t) + B_L(t)}{2} \quad (7)$$

When the matrix converter has  $m$ -phase ( $m=2,3,\dots$ ) output voltages, the input voltage range can be maximized by adding a common mode periodical term to increase the positive maxima and lower the negative minima.

Fig. 4 shows the input range optimization process to increase the magnitude of the output voltages. In Fig. 4, all the waveforms are normalized with reference to the amplitude of the input phase voltages. As seen in Fig. 4, the width of input range fluctuates with the ripple frequency of  $6f_i$  where  $f_i$  is the input frequency. Therefore, the possible range of the output voltage will have the maximum of 1.5. This means that, when considering only the input range optimization, the maximum amplitude of the output voltage can be 0.75 with reference to the

amplitude of the input phase voltages,  $V_s$ , and thus the input-to-output magnitude gain,  $q$ , is 0.75.

On the other hand, as seen in Fig. 5, a common mode term can be added to lower the maxima of the output voltage upper bound and increase the minima of the output voltage lower bound, allowing for greater amplitude output phase-to-phase difference to fit into the input range.

Applying only the input range optimization, the maximum magnitude of the output phase voltages is

$$V_{o,max(I.R.O)} = \frac{3}{4} V_s \tag{8}$$

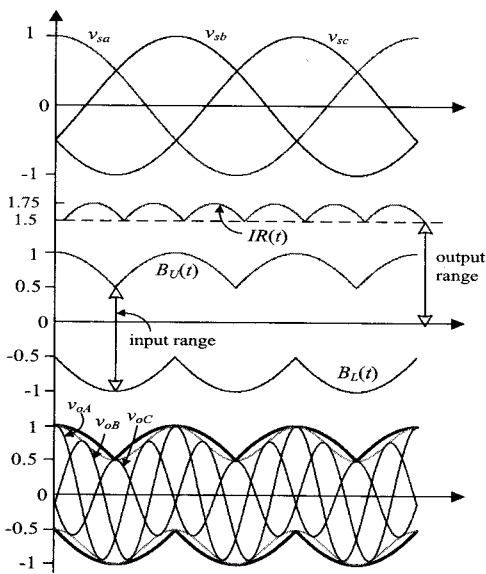


Fig. 4. Input voltage optimization.

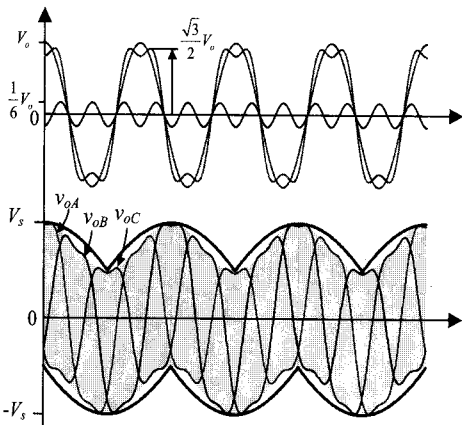


Fig. 5. Output voltage optimization.

If the output range optimization is additionally applied, the maximum magnitude of the output phase voltages is more increased as follows:

$$V_{o,max(O.R.O)} = \frac{\sqrt{6}}{3} V_o \tag{9}$$

where  $V_o$  is the output voltage amplitude before the output range optimization is applied.

#### 4. Application of DDPWM to various matrix converters

##### 4.1 3-phase to single-phase matrix converter

Fig. 6 shows the circuit configuration of a 3-phase to single-phase 1-leg matrix converter with a neutral connection. As seen in Fig. 7, both input range optimization and output range optimization cannot be applicable because a common mode voltage cannot be canceled out. The reference output voltage,  $v_{oA}^*$ , is

$$v_{oA}^* = q \cdot V_s \cos(\omega t) \tag{10}$$

As far as the maximum voltage conversion ratio,  $q_{max}$ , is concerned, it is limited to 0.5

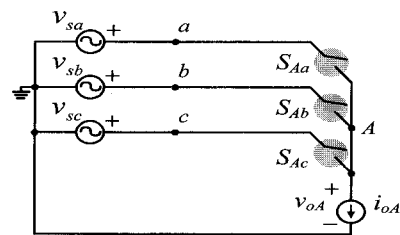


Fig. 6. Circuit configuration of a 3-phase to single-phase matrix converter with single-leg.

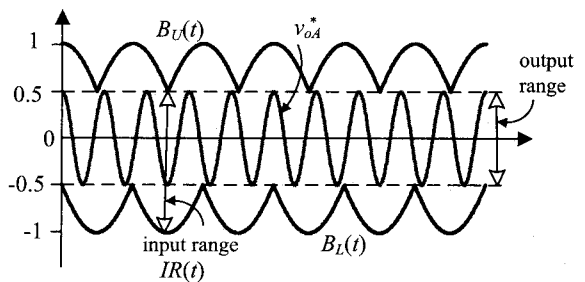


Fig. 7. Generation of reference output voltage in a 3-phase to single-phase matrix converter with 1-leg.

Fig. 8 shows the circuit configuration of a 3-phase to single-phase 2-leg matrix converter without a neutral connection [12]. It should be noticed that the two output phases may be separately controlled to follow their references. Normally, however, the two output phase voltage commands for each leg are given by:

$$\begin{aligned} v_{oA}^* &= q \cdot V_s \cos(\omega_o t) + \frac{1}{4} V_s \cos(\omega_i t) \\ v_{oB}^* &= q \cdot V_s \cos(\omega_o t - \pi) + \frac{1}{4} V_s \cos(\omega_i t) \end{aligned} \quad (9)$$

where  $v_{oA}^*$  and  $v_{oB}^*$  are the output phase voltage commands for A-phase and B-phase, respectively and  $\omega_i$  is the angular frequency of the input voltage. In this matrix converter, the input range optimization can be applicable but the output range optimization cannot be done. So, the maximum gain of  $q$ ,  $q_{max}$ , is equal to 0.75 for each phase.

#### 4.2 3-phase to 2-phase matrix converter

The 2-phase matrix converter may be suitable for two-phase loads, such as symmetrical two-phase induction motors or conventional single-phase machines with main and auxiliary windings [13-14].

Fig. 9 shows a 3-phase to 2-phase matrix converter with a neutral connection which will support the unbalanced current in the output. The output voltage commands can be given by:

$$\begin{aligned} v_{oA}^* &= q_A \cdot V_s \cos(\omega_o t) \\ v_{oB}^* &= q_B \cdot V_s \cos(\omega_o t - \varphi) \end{aligned} \quad (10)$$

where  $q_A$  and  $q_B$  are the voltage conversion ratios for the output A- phase and B-phase respectively and  $\varphi$  the displacement angle in the output phase voltages. It is worth noting that the maximum of  $q_A$  and  $q_B$  will also be 0.5 due to the neutral connection. That is,  $0 < q_A < 0.5$  and  $0 < q_B < 0.5$ . Additionally,  $\varphi$  can be an arbitrary value because the DDPWM implies a per-output-phase modulation feature.

Fig. 10 shows the circuit topology of a two-phase system including a 2-phase 3-leg matrix converter. The additional leg ( $S_{Ca}$ ,  $S_{Cb}$ ,  $S_{Cc}$ ) can be utilized to support unbalanced load currents. This converter is capable of generating output waveforms with higher magnitude compared to the 2-phase 2-leg matrix converter.

For the output phase voltage commands, input range optimization can be done. However, because the two phase outputs,  $v_{oA}$  and  $v_{oB}$ , may have an arbitrary phase difference, the positions of maxima and minima in the output phase voltage are not correlated so that the output range optimization cannot be applied.

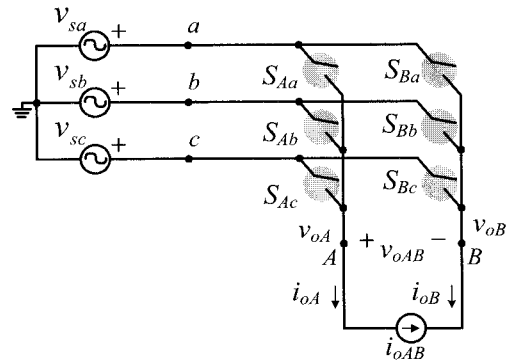


Fig. 8. Circuit configuration of a 3-phase to single-phase matrix converter with 2-leg.

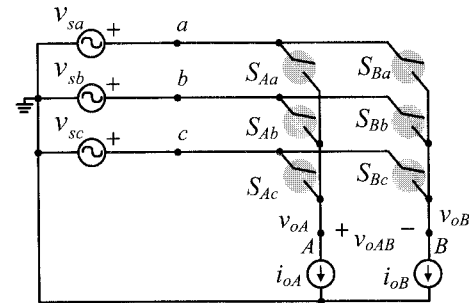


Fig. 9. Circuit configuration of a 3-phase to 2-phase matrix converter with 2-leg.

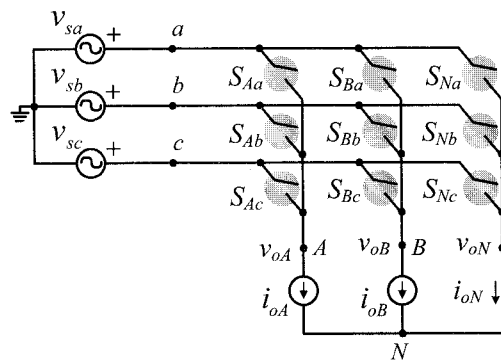


Fig. 10. Circuit configuration of a 3-phase to 2-phase matrix converter with 3-leg.

As a result, output voltage commands for the three-leg matrix converter will be:

$$\begin{aligned} v_{oA}^* &= q_A V_s \cos(\omega_o t) + \frac{1}{4} \cos(\omega_i t) \\ v_{oB}^* &= q_B V_s \cos(\omega_o t - \varphi) + \frac{1}{4} \cos(\omega_i t) \\ v_{oN}^*(t) &= +\frac{1}{4} \cos(\omega_i t) \end{aligned} \quad (11)$$

For the 2-phase 3-leg matrix converter,  $0 < q_A < 0.75$  and  $0 < q_B < 0.75$  to guarantee full range operation of  $\varphi$ .

### 4.3 3-phase to 3-phase matrix converter

Fig. 11 shows the circuit configuration of a common 3-phase to 3-phase matrix converter. The DDPWM has been well developed to modulate this converter. The input current synthesis can be performed by properly adjusting  $n$ , while maintaining  $T_s$  at a constant value. In this matrix converter, both input range optimization and output range optimization can be applicable because all common mode voltages can be canceled out. Therefore, the three output phase voltage references can be expressed by:

$$\begin{aligned} v_{oA}^* &= q \cdot V_s \cos(\omega_o t) + f(t) \\ v_{oB}^* &= q \cdot V_s \cos(\omega_o t - 2\pi/3) + f(t) \\ v_{oC}^* &= q \cdot V_s \cos(\omega_o t + 2\pi/3) + f(t) \end{aligned} \quad (12)$$

The sinusoidal output references ride on a common mode voltage,  $f(t)$ , which is given by

$$f(t) = \frac{1}{4} V_s \cos(3\omega_o t) - \frac{1}{6} \cdot q \cdot V_s \cos(3\omega_o t) \quad (13)$$

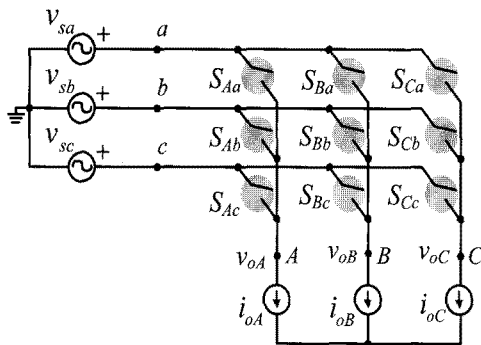


Fig. 11. Circuit configuration of a 3-phase to 3-phase matrix converter with 3-leg.

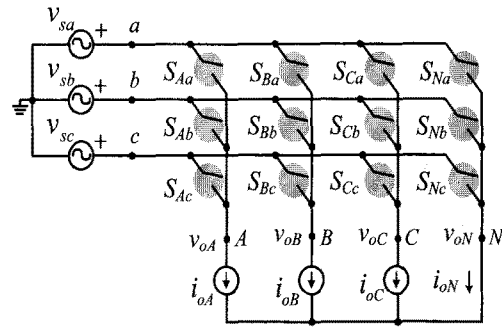


Fig. 12. Circuit configuration of a 3-phase to 3-phase matrix converter with 4-leg.

Fig. 12 shows the circuit configuration of a 3-phase 4-leg matrix converter. The DDPWM method can be used to modulate such a converter to generate three-phase output voltages/currents whose magnitudes are independently controlled. The 4-leg converter can be applied to drive any 3-phase loads, regardless of balanced and unbalanced loads. It can also be utilized in power conversion and generation systems with 3-phase 4-wire configuration [15]. Because both input range optimization and output range optimization can be applicable, the output references are given by:

$$\begin{aligned} v_{oA}^* &= q_A \cdot V_s \cos(\omega_o t) + f(t) \\ v_{oB}^* &= q_B \cdot V_s \cos(\omega_o t - 2\pi/3) + f(t) \\ v_{oC}^* &= q_C \cdot V_s \cos(\omega_o t + 2\pi/3) + f(t) \\ v_{oN}^* &= f(t) = \frac{1}{4} V_s \cos(3\omega_o t) - \frac{1}{6} \cdot q_x \cdot V_s \cos(3\omega_o t) \end{aligned} \quad (16)$$

where  $q_x = \max(q_A, q_B, q_C)$  and  $q_x$  has a maximum of 0.866.

## 5. Experiment Results

To verify the feasibility of the presented DDPWM methods for various matrix converter topologies, an experimental setup was built and the DDPWM controller was implemented using a TMS320VC33 DSP from Texas Instruments and an Altera CPLD (Manufacturer Part No: EP1K100QC208-1). Some of the hardware parameters are listed as follows:

$$\begin{aligned} V_{s-rms} &= 220 \text{ V}, C_f = 60 \text{ } \mu\text{F}, L_f = 100 \text{ } \mu\text{H}, f_i = 60 \text{ Hz}, \\ f_s &= 5 \text{ kHz}, R = 20 \text{ } \Omega, L = 50 \text{ mH}, \end{aligned}$$

where  $V_{s-rms}$  is the rms value of the input line-to-line voltage and  $C_f$  and  $L_f$  are the input filter capacitance and inductance respectively and  $R$  and  $L$  are the per-phase resistance and inductance in load respectively and finally  $f_s$  is the switching frequency.

Fig. 13 shows the experimental waveforms for the single-phase matrix converter seen in Fig. 6, where the voltage gain  $q$  is 0.5 and the output frequency  $f_o = 90$  Hz.

Fig. 14 shows the experimental waveforms for the single-phase 2-leg matrix converter in Fig. 8. The output voltage command is given by (10), in which both  $q_A$  and  $q_B$  are 0.5 and  $f_o = 90$  Hz. As seen in the waveforms in Fig. 13 and Fig. 14, the presented DDPWM method is able to modulate the single-phase matrix converter effectively.

Fig. 15 shows the experimental waveforms for the 2-phase 2-leg matrix converter (Fig. 9) under the conditions where  $\varphi = 90^\circ$ ,  $f_o = 30$  Hz,  $q_A = 0.5$  and  $q_B = 0.3$ . Fig. 16 includes the experimental waveforms for the 2-phase 3-leg matrix converter (Fig. 10) under the conditions where  $\varphi = 90^\circ$ ,  $f_o = 30$  Hz,  $q_A = 0.75$  and  $q_B = 0.5$ . The experimental waveforms in Fig. 15 and Fig. 16 confirm that the proposed DDPWM modulation strategy is capable of controlling a two-phase matrix converter with the desired voltage conversion ratios.

Fig. 17 shows the steady state experimental waveforms of output line-to-line voltage  $v_{oAB}$ , output current  $i_{oA}$ , input phase voltage  $v_{sa}$  and input current  $i_{sa}$  for a common 3-phase 3-leg matrix converter. The experimental conditions are  $q = 0.866$  and  $f_o = 40$  Hz. In Fig. 17,  $i_{sa}$  shows a small phase difference with leading power factor because of the input filter. It can be confirmed that the proposed direct PWM method is able to effectively synthesize both the output voltage and input current under unit input power factor.

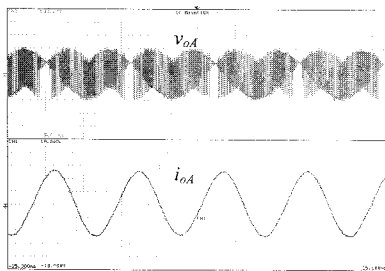


Fig. 13. Experimental waveforms for single-phase single-leg matrix converter. ( $v_{oA}$ : 100 V/div, 5 ms/div;  $i_{oA}$ : 1 A/div, 5 ms/div)

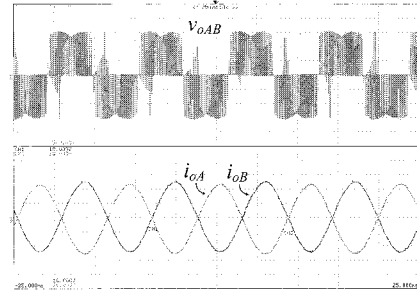


Fig. 14. Experimental waveforms for single-phase 2-leg matrix converter. ( $v_{oAB}$ : 100 V/div, 5 ms/div;  $i_{oA}$ : 2 A/div, 5 ms/div;  $i_{oB}$ : 2 A/div, 5 ms/div)

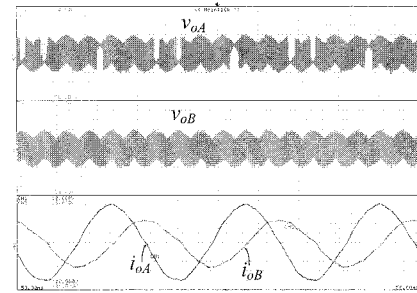


Fig. 15. Experimental waveforms for 2-phase 2-leg matrix converter. ( $v_{oA}$ ,  $v_{oB}$ : 100 V/div, 10 ms/div;  $i_{oA}$ ,  $i_{oB}$ : 1 A/div, 10 ms/div)

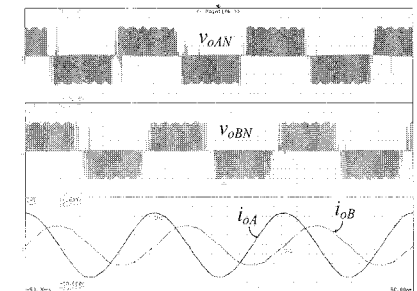


Fig. 16. Experimental waveforms for 2-phase 3-leg matrix converter. ( $v_{oAN}$ ,  $v_{oBN}$ : 100 V/div, 10 ms/div;  $i_{oA}$ ,  $i_{oB}$ : 2 A/div, 10 ms/div)

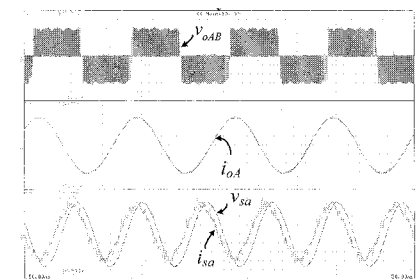


Fig. 17. Experimental waveforms for 3-phase 3-leg matrix converter. ( $v_{oAB}$ : 100 V/div, 10 ms/div;  $i_{oA}$ : 2 A/div, 10 ms/div;  $v_{sa}$ : 50 V/div, 10 ms/div;  $i_{sa}$ : 2 A/div, 10 ms/div)

Fig. 18 and Fig. 19 show experimental waveforms that reveal dynamic performance when  $f_o$  is changed from 30 Hz to 90 Hz and vice versa, respectively. In Fig. 18 and Fig. 19,  $q$  remains 0.866. It can be seen from Fig. 18 and Fig. 19 that the  $A$ -phase output current  $i_{oA}$  changed from 7 A to 4 A as theoretically expected. Because the three-phase  $R-L$  load is connected, the magnitude of the output current is decreased as the operating frequency increases.

The experimental results for the 3-phase 4-leg matrix converter (Fig. 12) are shown in Fig. 20. The experimental conditions are  $f_o = 30$  Hz,  $q_A = q_B = 0.866$  and  $q_C = 0.5$ . It can be confirmed from the experimental waveforms that the DDPWM approach is an effective way to modulate the 4-leg matrix converter.

## 6. Conclusions

In this paper, control strategy of various topologies of matrix converters is presented, which is based on the DDPWM. Because the DDPWM method has the characteristics of the inherent per-phase modular structure, it can be effectively applied to single-phase, two-phase and three-phase four-leg matrix converters as well as the common three-phase to three-phase matrix converter. Also, this paper treats command generation method in each matrix converter. The feasibility and validity of the proposed method has been verified by experimental results. Finally, it can be concluded that the presented method offers a very simple and effective way to modulate matrix converters.

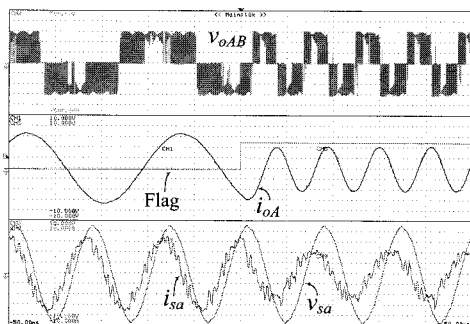


Fig. 18. Experimental waveforms for 3-phase 3-leg matrix converter when  $f_o$  is changed from 30 Hz to 90 Hz. ( $v_{oAB}$ : 100 V/div, 10 ms/div;  $i_{oA}$ : 2 A/div, 10 ms/div;  $v_{sa}$ : 40 V/div, 10 ms/div,  $i_{sa}$ : 2 A/div, 10 ms/div)

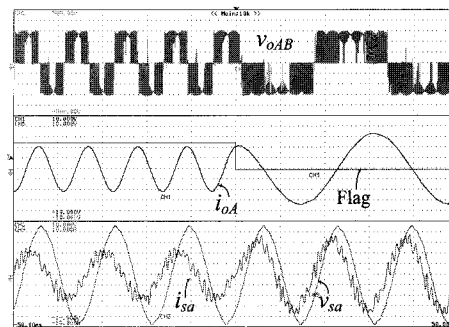


Fig. 19. Experimental waveforms for 3-phase 3-leg matrix converter when  $f_o$  is changed from 90 Hz to 30 Hz. ( $v_{oAB}$ : 100 V/div, 10 ms/div;  $i_{oA}$ : 2 A/div, 10 ms/div;  $v_{sa}$ : 40 V/div, 10 ms/div,  $i_{sa}$ : 2 A/div, 10 ms/div)

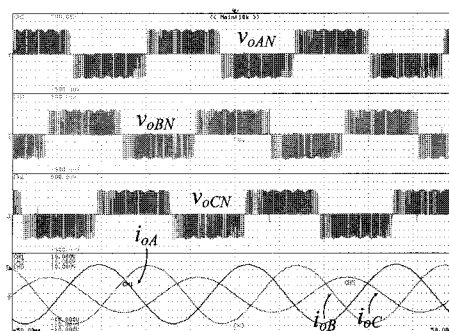


Fig. 20. Experimental waveforms for 3-phase 4-leg matrix converter. ( $v_{oAN}$ ,  $v_{oBN}$ ,  $v_{oCN}$ : 100 V/div, 10 ms/div;  $i_{oA}$ ,  $i_{oB}$ ,  $i_{oC}$ : 2 A/div, 10 ms/div)

## Acknowledgment

This work was supported by KESRI (R-2005-B-136), which is funded by MOCIE (Ministry of Commerce, Industry and Energy).

## References

- [1] H.-H. Lee, H.M. Nguyen, and T.-W. Chun, "Implementation of direct torque control method using matrix converter fed induction motor," *Journal of Power Electronics*, Vol. 8, No. 1, pp. 74-80, 2008.
- [2] L. Zhang, C. Watthanasarn, "A matrix converter excited doubly-fed induction machine as a wind power generator," *Conf. Record of Power Electronics and Variable Speed Drives*, pp. 532-537, Sep., 1998.
- [3] Byung-Moon Han, Yulong Li and Nam-Sup Choi, "Wind power system using doubly-fed induction generator and matrix converter," *Conf. Record of Korea-Japan Joint Technical Workshop on Semiconductor Power Converter*,



pp. 37-42, Sep., 2008.

- [4] P.W. Wheeler, J.C. Clare, D. Katsis, L. Empringham, M. Bland, T. Podlesak, "Design and construction of a 150KVA matrix converter induction motor drive," *Conf. Record of Power Electronics, Machines and Drives (PEMD)*, pp. 719-723, 2004.
- [5] A. Alesina and M. Venturini, "Solid-state power conversion: A fourier analysis approach to generalized transformer synthesis," *IEEE Trans. Circuits Syst.*, Vol. 28, No. CS-4, pp. 319-330, 1981.
- [6] A. Alesina and M. Venturini, "Analysis and design of optimum-amplitude nine-switch direct AC-AC converters," *IEEE Trans. Power Electron.*, Vol. PE-4, No. 1, pp. 101-112, 1989.
- [7] L. Huber and D. Borojevic, "Space vector modulated three-phase to three-phase matrix converter with input power factor correction," *IEEE Trans. Ind. Appl.*, Vol. 31, No. 6, pp. 1234-1246, 1995.
- [8] Domenico Casadei, Giovanni Serra, Angole Tani and Luca Zarri, "Matrix converter modulation strategies: a new general approach based on space-vector representation of the switch state", *IEEE Trans. Ind. Appl.*, Vol. 49, No. 2, pp. 370-381, 2002.
- [9] Young-Doo Yoon and Seung-Ki Sul, "Carrier-based modulation technique for matrix converter," *IEEE Trans. Power Electron.*, Vol. 21, No. 6, pp. 1691-1703, 2006.
- [10] Yulong Li, Nam-Sup Choi, Byung-Moon Han, Kyung-Min Kim, Buhm Lee and Jun-Hyub Park, "Direct duty ratio pulse width modulation method for matrix converters," *International Journal of Control, Automation, and Systems*, Vvol. 6, No. 5, pp.660-669, 2008.
- [11] Yulong Li and Nam-Sup Choi, "Carrier based pulse width modulation for matrix converters," *Conf. Record of IEEE Applied Power Electronics Conference*, pp.1709-1715, Feb. 15-19, 2009.
- [12] A. Zuckerberger, D. Weinstock and A. Alexandrovitz, "Single-phase matrix converter," *IEE Proceedings Electric Power Application*, Vol. 144, No. 4, pp. 235-240, 1997.
- [13] Sangshin Kwak, and Hamid A. Toliyat, "Development of modulation strategy of two-phase ac-ac matrix converters," *IEEE Trans. Energy Convers.*, Vol. 20, No. 2, pp. 493-494, 2005.
- [14] Sangshin Kwak, and Hamid A. Toliyat, "Direct ac/ac covnerters with 2 legs and 3 legs for two-phase systems," in *37th IEEE PESC Conf.*, pp. 1-5, 2006.
- [15] Wheeler, P. W. Zanchetta, P. Clare, J. C. Empringham, L. Bland, M. and Katsis, D., "A utility power supply based on a four-output leg matrix converter," *IEEE Trans. Ind. Electron.*, Vol. 44, No. 1, pp. 174-186, 2008.



**Yulong Li** was born in China, in 1982. He received his B.S. degree in Communication Engineering from Beijing University of Petro-chemical Technology, China, in 2004, and his M.S. and Ph.D. degrees in Electrical Engineering from Chonnam National University, Yeosu, Korea in 2006 and 2009, respectively. Currently, he is with Hyundai Heavy Industries Co., LTD., Korea as a researcher. His research interests are in the areas of modeling and control of power electronics converters and renewable generations. He is also is a member of the Korean Institute of Power Electronics.



**Nam-Sup Choi** was born in Seoul, Korea, in 1963. He received his B.S. degree in Electrical Engineering from Korea University in 1987. He received his M.S. and Ph.D. degrees in Electrical Engineering from the Korea Advanced Institute of Science and Technology (KAIST), Taejeon, Korea in 1989 and 1994, respectively. He is currently a professor in the Division of Electrical, Electronic Communication and Computer Engineering, Chonnam National University, Yeosu, Korea. His research interests include the modeling and analysis of power conversion systems, matrix converters and multilevel converters for renewable energy systems and micro-grid applications.



**Byung-Moon Han** received his B.S. degree in Electrical Engineering from Seoul National University, Korea in 1976, and his M.S. and Ph.D. degrees from Arizona State University in 1988 and 1992, respectively. He was with Westinghouse Electric Corporation as a senior research engineer in the Science & Technology Center. Currently he is a professor in the Department of Electrical Engineering at Myongji University, Korea. His research interests include power electronics applications for FACTS, custom power and distributed power generation.